

Investigation on temperature fields in industrial chilling of pork legs for PDO Parma ham production and coupled temperature/microbial growth simulation

Massimiliano Rinaldi¹ · Matteo Cordioli¹ · Davide Barbanti¹

Revised: 18 October 2016 / Accepted: 28 October 2016 / Published online: 10 January 2017
© Association of Food Scientists & Technologists (India) 2017

Abstract In the present work, temperature distribution within an industrial blast chiller with pork leg for Protected Designation of Origin Parma ham production was studied and the slowest cooling zone and the fastest cooling zone were recognized. Moreover, apparent heat transfer coefficients in both positions were calculated and resulted equal to 27.1 and 15.6 W m⁻² °C⁻¹, respectively. A finite element method model by distinguishing the three main components (skin, lean meat and bone) of the leg for the unsteady heat transfer during cooling was developed and validated against industrial chiller data. Good agreement between experimental and simulated data was obtained with RMSE value for thermal centre equal to 0.81 °C. Furthermore, in order to introduce CCP limit in the HACCP plan, a microbial growth model of the most important pathogens in meat was developed starting from the heat transfer model results. Temperature as well as pathogen growth were estimated in the case of different plant breakdowns. Defined CCP limit was represented by reaching 11 °C at 5 mm of depth within 2 h from the beginning of the cooling process, moreover a different cooling program was simulated and established as the alternative one.

Keywords Parma ham · Chilling process · FEM modelling · Microbial growth modelling

Introduction

Bacterial contamination of fresh meats can occur during normal slaughter and handling procedures, although this contamination can be minimized by adherence to good hygienic practices during slaughter as reported in Ministerial Decree No. 253/1993. Chilling, either by forced air or water spray systems, is universally used to reduce the growth of both pathogenic and spoilage bacteria on animal carcasses. In particular, Protected Designation of Origin (PDO) Parma ham Code of Rules (Ministerial Provision of 03/03/2014) requires that the core temperature of pork legs should be reduced from about 40 to 0/2.5 °C within 24 h and before any cutting process occurs. Cooling large pieces of meat such as legs in short time is a challenge for the meat industry and could be very expensive in terms of energy consumption (Ramírez et al. 2006).

Moreover, the EC Regulations number 852/2004 and 853/2004 (European Parliament & Council, 2004) stated that, unless other specific provisions provide otherwise, post-mortem inspection must be followed immediately by chilling in the slaughterhouse to ensure a temperature throughout the meat of not more than 3 °C for offal and 7 °C for other meat along a chilling curve that ensures a continuous decrease of the temperature. Moreover, food operators have to guarantee adequate ventilation in order to avoid condensation in the chilling room and on the surface of the meat as the bacteria are confined almost exclusively to the carcass surface (Adzitey and Nurul 2011) rather than to the deep muscle tissue.

Kondjoyan and Daudin (1997) demonstrated that the local values of the transfer coefficients could be very different from one location to another at the surface of a pork hindquarter. Thus, heat transfer rate deeply depends also on carcass location within industrial plant and for this reason

✉ Matteo Cordioli
matteo.cordioli@studenti.unipr.it

¹ Department of Food Science, University of Parma, Parco Area delle Scienze 47/A, 43124 Parma, Italy

temperature distribution study within industrial chiller is always required.

With the development of computer technology, the design of cooling processes underwent tremendous development. Use of advanced modelling techniques reduces the complexity in solving the non-linear partial differential equation of heat transfer, such reported by Rinaldi et al. (2014).

Several approaches were proposed to model the temperature evolution within meat carcasses during cooling process, since the work of Kuitche et al. (1996) with a model based on analytical solutions of unsteady heat transfer in elementary shapes, up to the model proposed by Pham et al. (2009) in which computational fluid dynamics (CFD) was used to estimate the local heat and mass transfer coefficients, assuming uniform surface temperatures, and a finite element grid was used to solve the heat transfer equation in the product, which has an elongated shape. In particular, Pham et al. (2009) during industrial tunnel tests reported unacceptable errors in temperature prediction due to uncertainties in the location of the thermocouples on the surface, uncertainties in air velocity and turbulence. Moreover, the industrial tests presented many variations from place to place due to several interferences with airflow.

Trujillo and Pham (2003) reported accurate predictions of the centre and surface temperature profiles of beef leg, loin and shoulder by means of an evolutionary algorithm, but no distinctions between bones, fat and lean meat thermal properties were done.

More recently, Kuffi et al. (2016) developed a computational fluid dynamics (CFD) model to predict the changes in temperature and pH distribution of beef carcass during chilling. The Authors measured the carcass temperatures at various depths and sections during a chilling experiment in commercial chiller conditions for model validation only in a single experiment and with one carcass.

Till date few scientific studies carried out on industrial plants were focused on pork leg chilling for PDO Parma ham production. In addition, as reported by Pham et al. (2009), the fat cover on the carcass' butt is very unpredictable, due to trimming of the surface fat by workers in that region. For these reasons, the aim of this work was to experimentally study the cooling process into industrial plant, to evaluate the homogeneity of air distribution and identify the slowest cooling zone (SCZ) and the fastest cooling zone (FCZ). Then, the obtained experimental data was employed to develop and validate a bi-dimensional transient heat transfer finite element model for the air blast cooling of pork leg for PDO Parma ham production. A further aim was the modelling of microbial growth on the leg surface by considering time-variable boundary conditions and the effects on this phenomenon of hypothetical plant breakdowns.

Heat exchange theory

Conductive heat transfer for isotropic food product is based on Fourier's Eq. (1):

$$\frac{\partial T}{\partial t} = \alpha \cdot \nabla^2 T \quad (1)$$

where α represents the thermal diffusivity value ($\text{m}^2 \text{s}^{-1}$) and relates the ability of a material to conduct heat to the ability to store it. Thermal diffusivity directly depends on food physical properties:

$$\alpha = \frac{k}{\rho \cdot c_p} \quad (2)$$

where ρ is material density (kg m^{-3}), k thermal conductivity ($\text{W m}^{-1} \text{K}^{-1}$) and c_p specific heat capacity ($\text{J kg}^{-1} \text{K}^{-1}$).

While ∇^2 is the Laplace's operator that will be different depending on the considered geometry; for a bi-dimensional sample, Eq. (1) becomes:

$$\frac{\partial T}{\partial t} = \alpha \cdot \left(\frac{\partial^2 T}{\partial x^2} + \frac{\partial^2 T}{\partial y^2} \right) \quad (3)$$

Generally, Eq. (3) can be solved by means of several methods such as finite difference, finite element and finite volumes, whose allow replacing a differential equation with a certain number of algebraic ones by discretising the variables from whom the studied function depends.

The initial condition is the uniform temperature within the whole volume of the object (Bergman et al. 2011):

$$T = T_{in} \text{ for time } t = 0$$

while the Dirichlet boundary condition of the first type was assumed with the entire boundary ($x = 0$) at a prescribed temperature:

$$T(0, 0, t) = T_{in} \text{ and } T(x, 0, t) = T(y, 0, t) = T_s$$

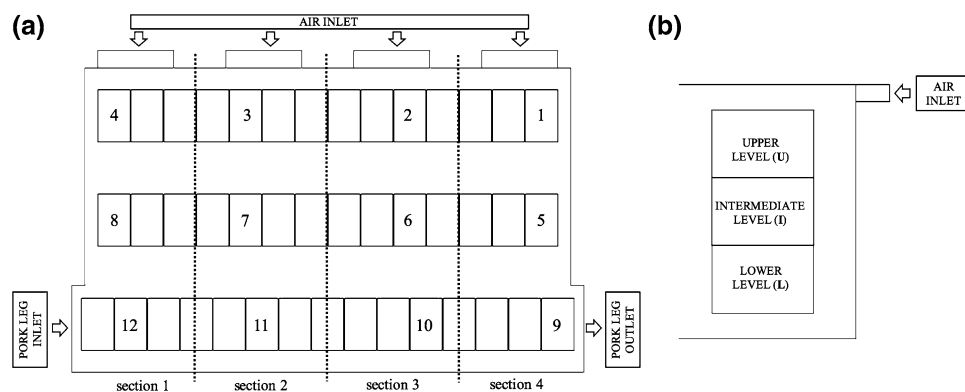
in this case the temperature imposed on the surface of the pork leg was equal to that experimentally measured in each position.

Materials and methods

Samples and chilling plant

The experimental measurements were carried out in an industrial blast chiller with an air velocity at the fans' exit of 5 m s^{-1} and that contained 1290 legs: the duration of the chilling process was 22.5 h. Industrial refrigerating room presented 3 tracks, 2 of them with 14 and the remaining with 15 trolleys, each trolley had 3 levels and contained about 10 legs per level. A schematically representation of

Fig. 1 Distribution of the temperature probe inside the chilling room: **a** (plan) trays chosen for the temperature measurement and **b** (side view) levels inside each tray



the plant was reported in Fig. 1: panel (a) shown the room plant while panel (b) shown the vertical structure of the trolley. Legs mean initial weight was about 19 kg and at the end of the chilling process mean weight loss was about 1.4%. Standard chilling program presented three steps: 3.5 h at 2 °C (STEP 1), 7 h at 0 °C (STEP 2) and finally, 12 h at -3 °C (STEP 3). During the leg cooling process two defrosting steps, without air renewal, were planned at about 3 and 10 h after the beginning of the procedure.

Temperature, humidity and pH measurement

The temperatures were measured, with an acquisition interval of 5 min, by means of wireless temperature loggers (Ebro Electronic GmbH & Co, Ingolstadt, Germany) on 12 different trolleys and at 3 different positions for each trolley (one for each levels) in the refrigerating room, in order to identify the slowest cooling zone (SCZ) and the fastest cooling zone (FCZ). The distribution of the thermocouples inside the room is reported in Fig. 1. Five repeated cooling treatments were performed with the temperature loggers in the same position in order to evaluate the average temperatures and standard deviations of the measurement; moreover, data from repetitions were statistically compared by means of one-way ANOVA and no significant differences were observed. The overall coefficient of variation (standard deviation/average temperature * 100) at all measurement points resulted lower than 5% and hence, for a clear reading, in figures only average values (without error bars) are reported.

Then, to experimentally quantify the cooling curve inside the leg in the SCZ and FCZ, the temperatures were measured by means of 3 data loggers positioned near the geometric centre, near the surface (at 5 mm under the skin) of the leg and in a position near the leg to measure the air temperature. Four repetitions for each position were performed and, also in this case, the overall coefficient of variation resulted lower than 5% and hence only average values are reported.

The heat transfer coefficient in SCZ and FCZ positions was estimated by means of the energy balance at the

sample surface, with a simplified form of the mixed Dirichlet–Neumann’s or Robin’s boundary condition:

$$-k \cdot A \cdot \left(\frac{dT}{dr} \right)_{r=R} = h \cdot A \cdot (T_s - T_\infty) \quad (4)$$

where k is thermal conductivity ($\text{W m}^{-1} \text{ }^\circ\text{C}^{-1}$), A is the sample surface area (m^2), h the convective heat transfer coefficient ($\text{W m}^{-2} \text{ }^\circ\text{C}^{-1}$), T_s the leg surface temperature ($^\circ\text{C}$) and T_∞ the heating fluid temperature out of the boundary layer ($^\circ\text{C}$). The evaporation-based term was not considered as weight loss resulted very low and mainly in the last part of the process due to the high relative humidity inside the chamber.

Relative humidity within the cooling room was also measured every 2 h by means of a digital thermo hygrometer (Giorgio Bormac S.r.l, Carpi, Modena, Italy), positioned inside a trolley at the intermediate level. The humidity values were recorded during the entire cooling treatment, therefore five repeated measurements were performed and the average values are reported in the results.

pH was measured every hour in all the legs of the levels considered for the temperature measurement, for an amount of 360 measure (10 leg for each level, 3 levels for each position and 12 positions inside the chilling room). The measures were performed by means of a portable pH-meter (Knick Elektronische Messgeräte GmbH & Co, Berlin, Germany) in correspondence of hamstring muscle as reported in PDO Parma guidelines (Ministerial Provision of 03/03/2014).

Heat transfer model development

A 2-D model, based on finite element solution of unsteady state conductive heat transfer with variable time–temperature boundary conditions, for simulation of pork legs heat transfer during industrial blast chilling was developed. The finite element (FE) commercial code COMSOL[®] 2008 (Stockholm, Sweden) was employed to solve the system of partial differential equations.

Leg section geometry was obtained by means of several pictures taken from samples: the largest leg section was approximated to an ellipse with the major axis of 400 mm and the minor axis of 280 mm. The skin and fat were positioned around the entire leg, with a thickness of 15 mm; the bone, approximated to a circle with a diameter of 80 mm, was positioned near the bottom, with the centre at a distance of 190 mm from the upper surface. The model geometry, after a preliminary mesh independent analysis, was discretized into 804 triangular meshes.

The thermal and physical properties (thermal conductivity k , heat capacity c_p and density ρ) of the three main components were found in the literature (James and James 2002):

$$\begin{aligned} \text{Skin and fat } k &= 0.21 \text{ W m}^{-1} \text{ K}^{-1}; c_p \\ &= 4755 \text{ J kg}^{-1} \text{ }^\circ\text{C}^{-1}, \rho = 920 \text{ kg m}^{-3}; \end{aligned} \quad (5)$$

$$\begin{aligned} \text{Lean muscle } k &= 0.49 \text{ W m}^{-1} \text{ K}^{-1}; c_p \\ &= 3060 \text{ J kg}^{-1} \text{ }^\circ\text{C}^{-1}, \rho = 1070 \text{ kg m}^{-3}; \end{aligned} \quad (6)$$

$$\begin{aligned} \text{Bone } k &= 0.26 \text{ W m}^{-1} \text{ K}^{-1}; c_p = 2850 \text{ J kg}^{-1} \text{ }^\circ\text{C}^{-1}, \rho \\ &= 1330 \text{ kg m}^{-3}. \end{aligned} \quad (7)$$

In this study, a transient simulation was carried out and a uniform time varying temperature condition was applied to the external surface of the leg. For the model validation, time–temperature profiles imposed on the external surface of the leg were obtained from the value measured near the leg surface in experimental tests. For the simulation of different processing conditions, the different time–temperature profiles reported in Table 3 were imposed.

Thermal model validation

The model was then validated by comparing predicted and experimental temperature data; differences between simulated and experimental curves were estimated by means of root mean square error (RMSE), with the following:

$$\text{RMSE} = \sqrt{\frac{\sum_{i=1}^n (T_E - T_P)^2}{N}} \quad (8)$$

where T_P is simulated temperature and T_E is measured temperature, at time t .

Microbial growth modelling

In addition, microbial growth of the most important pathogenic bacteria (*Listeria monocytogenes*, *Salmonella spp.*, *Yersinia enterocolitica* and *Escherichia coli*) was modelled by means of USDA pathogen modelling program

(PMP v. 7.0) by using the actual temperature profile of the leg showing to be in the worst position within the room. PMP is a package of models that can be used to predict the growth and inactivation of foodborne bacteria and primarily pathogens, under various environmental conditions. The models are based on experimental data of microbial behaviour in liquid microbiological media and food. The software can permit to choose the microorganism to model, the environmental conditions such as temperature, pH, water activity and sodium nitrate. When the initial contamination was inserted the software can predict the growth curve of microorganism.

Statistical analysis

Means and standard deviations (SD) were calculated with STATISTICA (release 8.0, Statsoft Inc., Tulsa, Oklahoma, USA) statistical software. To identify differences of pH among samples was applied one-way-analysis of variance (ANOVA) and least significant difference test (LSD) at a 95% confidence level ($P \leq 0.05$).

Results and discussion

Temperature distribution inside chiller

The experimental results showed great differences in the air temperatures near the pork legs between the 36 considered positions. To simplify the system, only the upper level was taken into consideration since the hot air goes upward and the other levels were considered colder. By analysing the 12 temperature profiles of the upper level, shown in Fig. 2, the slowest cooling zone (SCZ) inside the chiller resulted located in the position 2 U. Starting from this result, it was chosen to find the fastest cooling zone (FCZ) in the same plant section of SCZ (section 3), in order to guarantee similar characteristics of the air flow: the FCZ resulted near the position 10 U. These results were in agreement with expectations, as the SCZ was located under the fan in a position hard to be reached by the airflow while the FCZ was positioned in front of the fan near the wall where the air recirculation was expected to be maximum. The mean difference in air temperature between the two positions during the whole cooling process resulted equal to 2.9 °C. During defrosting, as expected, air temperature in the neighbourhood of the pork leg increase of about 10 °C and 5 °C (Fig. 2) for the first and the second event, respectively. In Fig. 2 the relative humidity values along the cooling phase are also reported; it's possible to note an increase in relative humidity only in the first phase when the temperature inside the room was higher than the dew point temperature. These conditions favoured the formation

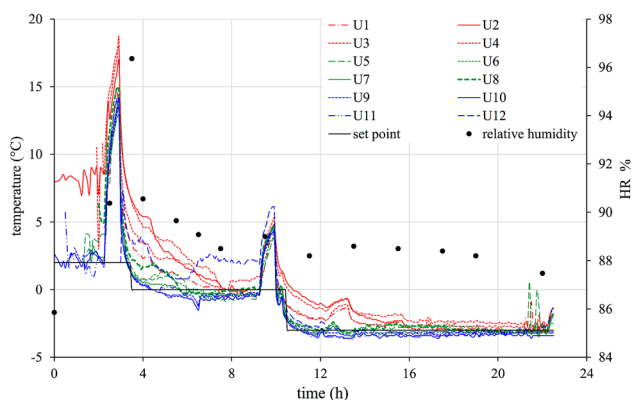


Fig. 2 Air temperature distribution among the considered positions (relative to the upper level) and chilling room relative humidity values

of condensate in the form of frost on convectors. With the two defrosting phases, the ice was removed from the chiller and the relative humidity was reduced and kept constant. Once checked the different cooling capacity inside the chiller room, the temperature profiles inside the pork leg located in the SCZ and the FCZ were studied.

Convective heat transfer coefficient at samples' surface in SCZ ($15.6 \pm 0.8 \text{ W m}^{-2} \text{ }^\circ\text{C}^{-1}$) and FCZ ($27.1 \pm 1.0 \text{ W m}^{-2} \text{ }^\circ\text{C}^{-1}$) positions resulted significant different probably due to the different temperature values at the surface (Fig. 2) or to the different air velocity depending both on position and distance from fans. Calculated values of convective heat transfer coefficients were similar to those reported in the literature: Kondjoyan (2006) calculated a value of heat transfer coefficient in food refrigeration ranging from 15 to $35 \text{ W m}^{-2} \text{ }^\circ\text{C}^{-1}$ for a range of air velocity of $1\text{--}5 \text{ m s}^{-1}$; similarly, h values of 10, 20 and $35 \text{ W m}^{-2} \text{ }^\circ\text{C}^{-1}$ were reported for meat food products for 0.6, 1.4 and 3.6 m s^{-1} (ASHRAE 2010).

Temperature distribution inside the leg

Once the fastest and the slowest cooling zone were identified in the inside chiller, the next step was to study the temperature profile inside pork legs in these positions. The temperature profile experimentally measured inside the pork leg at the SCZ (position 2 U) and at FCZ (position 10 U) appeared different (Fig. 3a) in all the three positions investigated for each leg. This result confirmed what reported in the previous paragraph: the great difference in the heat transfer coefficient at samples' surface of the two positions (2 U and 10 U) greatly affected the heat exchange inside the leg. To quantify the difference between the two positions, the time needed to reach a certain temperature was calculated, starting from the data obtained from the thermal centre. As reported in Table 1, samples at the

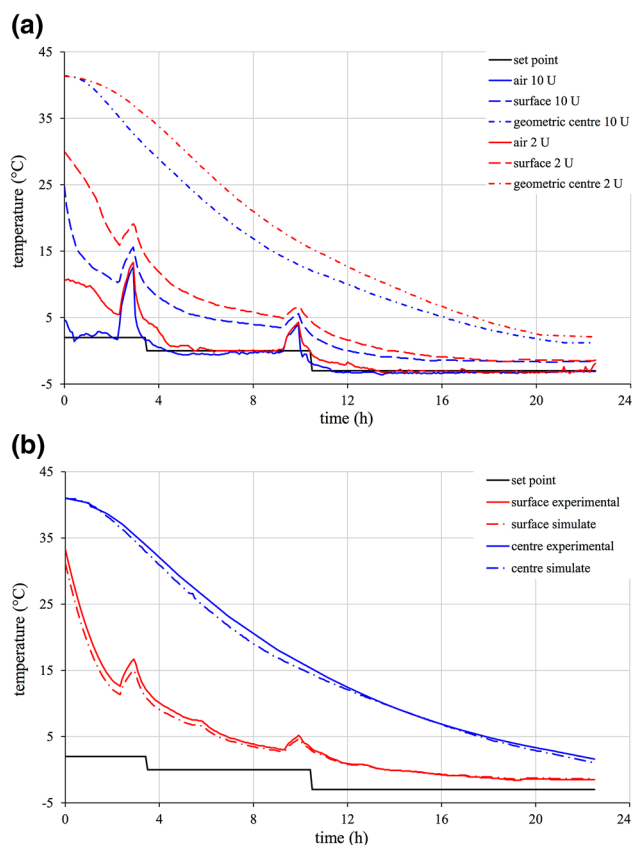


Fig. 3 a comparison of the temperature profile inside the leg (surface air, 5 mm of depth and leg centre) in the SCZ (2 U) and FCZ (10 U) positions. b Comparison between experimental and simulated temperature profiles at 5 mm of depth and at leg centre

Table 1 Cooling times (h) at leg centre in the two selected positions (mean \pm SD)

	Position	
	2 U	10 U
From 40 to 20 $^\circ\text{C}$	8.4 ± 0.8	6.8 ± 0.5
From 20 to 10 $^\circ\text{C}$	5.3 ± 0.4	5.3 ± 0.2
From 10 to 2.5 $^\circ\text{C}$	6.4 ± 0.4	6.9 ± 0.3
From 40 to 2.5 $^\circ\text{C}$	20.2 ± 0.9	19.0 ± 1.0

position 2 U took about 1.2 h more than sample 10 U to reach 2.5 $^\circ\text{C}$ (the minimum temperature value reported for the chilling process in PDO Parma Code of rules) and the main difference occurred in the first part of the cooling process (from 40 to 20 $^\circ\text{C}$). Such differences may be due either to the natural variability of the size and composition of the pork leg, or due to the combination of two factors:

- air flow, that was probably more homogenous and not hindered before reaching the position 10 U as it came directly from the convector. Conversely, in the position 2 U the air reached the product only after going through

other legs: this may cause a local slowdown of the flow velocity. This heterogeneity of air flow inside the cooling room was increased by the presence of zones at high and low air velocity where the heat exchange was reduced. This phenomenon could reduce the whole efficiency of the cooling process.

- Air temperature was lower around the position 10 U than the temperature around the position 2 U (Fig. 3a); this increase of the air temperature was due to the heat exchange between the pork legs (hot body) and the air flow (cold body) inside the plant. In the SHZ the air reached the leg after removing heat from many other legs, therefore the air reached the legs with a higher temperature with respect to the air at FCZ.

The combination of these two phenomena reduced the apparent thermal exchange coefficient of the pork leg in function of the disposition inside the cooling room. This fact leads to a different exchange rate inside the products and to a reduction of the efficiency and efficacy of the cooling process as consequence.

pH determination along the cooling process

Mean pH values varied from 6.41 ± 0.05 to 5.70 ± 0.02 with the greatest variations was observed in the first 6 h of cooling. The results were in good agreement with expectations for meat with no PSE (Pale Soft Exudative) or DFD (Dry Firm Dark) defects, where the final mean pH ranged from 5.5 to 6.0. PSE occurred when the pH of meat is <6 at 45 min after slaughter or a final pH < 5.3 . DFD is when the ultimate pH post mortem measured after 12–48 h is ≥ 6 (Adzitey and Nurul 2011). Leg pH variations before and after the cooling process were found to be not statistically correlated to the position into the cooling room, probably cause of the natural variability of this parameter.

Heat transfer model

The results obtained from the mathematical model were compared against experimental measurements carried out in the industrial plant for the two positions taken into account for the model development: only results for the SCZ corresponding to position 2 U are reported (Fig. 3b). Leg thermal centre was located in the lean meat just near the bone. The developed model allowed simulating with good approximation the temperature profile both at the thermal centre and at a depth of 5 mm under the skin both for position 2 U (Fig. 3b) and position 10 U (not shown). RMSE values obtained comparing experimental data with simulated ones for thermal centre and 5 mm depth were 0.81 and 0.75 °C, respectively. The difference between the model and the experimental tests could be due to:

- geometry of the domain as the leg section wasn't perfectly elliptical;
- sizing and positioning of the bone which it has been approximated to a cylinder;
- thickness of the fat layer as actually it wasn't homogeneous along the whole circumference;
- number of the mesh in the domain and time steps of the simulation chosen to reduce the effort of the calculation process.

Notwithstanding, good agreement between experimental and simulated curves was obtained and the developed mathematical models could be considered successfully validated for heat transfer.

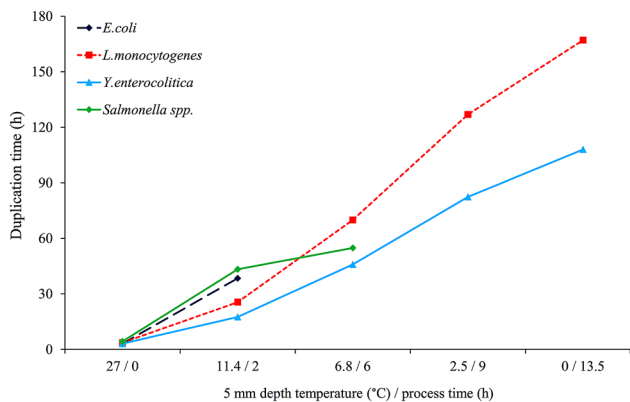
The developed model was then used to predict the temperature evolution in the pork legs due to variations in scheduled process. In this case, since the chilling chamber contained a great amount of product that could be damaged with a potential great economic injury, the only way to study new temperature profile in the mathematical modelling. Particularly, 10 variations were hypothesized with an increase of 1, 2, 3 and 4 h in STEP 1 and STEP 2 and other combinations in order to reduce the energy consumption of the process and to reduce the STEP 3 that could cause freeze damage to the surface of legs. For each variation, final temperature inside the product was calculated both in SCZ and FCZ (Table 2). Results of simulations showed that unfortunately have of the tested variations on STEP 1 and STEP 2 allowed having the same performance of the scheduled program and reducing the difference in core temperature between SCZ and FCZ. On the contrary, increasing STEP 3 allowed reducing time to reach the final core temperature as well as differences between SCZ and FCZ but surface temperature has to be monitored in order to avoid damages due to under zero temperatures.

Microbial growth modelling

Experimental leg temperature data recorded at 5 mm of depth were used to estimate duplication times of the most important pathogens for meat products (Fig. 4). Temperature profile at 5 mm of depth experimentally measured in the SCZ (position 2 U) for the actual scheduled cooling process gave high duplication times (Fig. 4) and allowed successfully containing growth of the considered microorganisms if no breakdowns happen. In addition, the developed heat exchange model was used to simulate the temperature profile in the same positions in case of plant breakdowns after 1 (B1), 2 (B2) and 6 (B6) hours from the beginning of the process and the simulated temperatures were used to estimate the duplication time of the most important pathogens. Duration of each breakdown was set

Table 2 Modelled final core temperatures in SCZ and FCS by varying scheduled process

	Duration (h)			Final T at core (°C)	
	STEP 1	STEP 2	STEP 3	FCZ	SCZ
Scheduled process	3.5	7	12	0.70	2.16
Var1	4.5	7	11	0.91	2.37
Var2	5.5	7	10	1.16	2.63
Var3	6.5	7	9	1.43	2.91
Var4	7.5	7	8	1.74	3.23
Var5	3.5	8	11	0.88	2.38
Var6	3.5	9	10	1.07	2.61
Var7	3.5	10	9	1.29	2.85
Var8	3.5	11	8	1.53	3.11
Var9	4.5	8	10	1.11	2.59
Var10	5.5	9	8	1.63	3.15
Var11	3.5	7	13	0.50	1.39
Var12	3.5	7	14	0.39	1.28
Var13	3.5	7	15	0.30	1.18
Var14	3.5	7	16	0.22	1.10

**Fig. 4** Duplication times of the most important pathogens for the scheduled chilling process

to 3 h and air temperature was considered equal to the last value before the plant stop.

Heat transfer modelling showed that temperature at 5 mm depth:

- in case of B1 increased from 20.0 to 21.5 °C along the first hour, then it tended to decrease in the remaining 2 h;
- for the case B2 the temperature increased from 9.0 to 10.2 °C in the first hour, then it tended to decrease toward the initial value for the remaining time;
- finally, for the case B6, the temperature value moved from 5.0 to 5.5 °C along the first hour, then it tended to return to the initial values.

Changes in duplication time of *Listeria monocytogenes* caused by considered plant breakdowns (B1, B2 and B6) are reported in Table 3. *Listeria monocytogenes* is a Gram-

Table 3 Duplication times with scheduled process versus breakdown with a duration of 3 h at 1 (B1), 2 (B2) and 6 (B6) hours after the process beginning

	Plant breakdown duration			
	No	1 h	2 h	3 h
<i>Listeria monocytogenes</i>				
B1	7.1	6.5	6.9	7.0
B2	37.1	29.3	33.2	35.3
B6	92.3	84.5	87.9	89.5
<i>Salmonella</i>				
B1	7.9	6.9	7.3	7.6
B2	49.3	46.3	47.3	48.5
B6	59.3	58.5	58.5	58.8
<i>Escherichia coli</i>				
B1	7.7	6.6	7.1	7.4
B2	77.4	57.4	64.9	71.8
<i>Yersinia enterocolitica</i>				
B1	5.1	4.7	4.9	5.0
B2	25.7	21.1	22.5	24.5
B6	64.5	58.5	60.8	63.2

positive, intracellular bacterial pathogen that causes illness and mortality in humans and livestock. It is a significant food-borne pathogen due its widespread distribution in nature, its ability to survive in a wide range of environmental conditions, and its ability to grow at refrigeration temperatures (WHO 1988). Karakolev (2009) reported an incidence of 5% of *Listeria monocytogenes* in raw pork meat for a 5-years period (2002–2007). The greatest variation for *Listeria monocytogenes* duplication times (Table 3) was obtained for the case B1, as expected; similar results were obtained for *Salmonella spp.*, *Yersinia enterocolitica* and *Escherichia coli*. From these results it's

possible to note that the greater danger for the pathogens development occurs when the breakdown of the plant takes place within the first hours of the process, because the estimated duplication time of the microorganism were much lower than the process duration.

Finally, the temperatures profiles data at 5 mm of depth and the duplication times of the food pathogens obtained through the mathematical models (in the standard process condition and in the case of breakdown events), were combined to introduce a critical control point (CCP) in the HACCP plan of the factory referred to the cooling process. Established critical limit for this CCP was reaching 11 °C at 5 mm depth within 2 h from the beginning of the cooling process. Several alternative cooling programs were studied to be used when CCP limit was not respected and centre and 5 mm depth temperature were simulated both in the SCZ and in the FCZ of the cooling room. Alternative cooling program with the best results was as follows: 9 h at 0 °C and finally 10 h at −3 °C. Alternative cooling program had to increase leg cooling rate but 5 mm depth temperature can't go under −2.5 °C as cold damages could appear in the leg surface, with particular reference to the meat not covered by means of the skin. This is not acceptable for a high quality product such as PDO Parma ham.

Conclusion

In the present work, temperature distribution within an industrial blast chiller was experimentally studied and slowest and fastest cooling positions were recognized as well as apparent heat transfer coefficients calculated. Moreover, a FEM model for the unsteady heat transfer in pork leg for PDO Parma ham production cooling was developed and validated against experimental data on an industrial chiller. The pork leg section was divided in the three main components (skin, lean meat and bone) and good agreement between experimental and simulated data was obtained. Developed model was used to simulate cooling program different from scheduled one in order to reduce times or energy consumption. In addition, microbial growing and temperature modelling were coupled in order to investigate temperature and pathogen growth in the case of plant breakdown. The obtained data was used to introduce a CCP limit for the HACCP plan and to create alternative cooling programs to be used in case of plant breakdown.

References

- Adzitey F, Nurul H (2011) Pale soft exudative (PSE) and dark firm dry (DFD) meats: causes and measures to reduce these incidences—a mini review. *Int Food Res J* 18:11–20
- ASHRAE (2010) Thermal properties of foods. In: 2010 ASHRAE handbook refrigeration, chapter 19. American Society of Heating, Refrigerating and Air-Conditioning Engineers, Atlanta, GA
- Bergman TL, Lavine AS, Incropera FP, DeWitt DP (2011) Fundamentals of heat and mass transfer. Wiley, New York
- EC Regulation No. 852/2004 of the European Parliament & of the Council of 29 April 2004
- EC Regulation No. 853/2004 of the European parliament & of the Council of 29 April 2004
- James SJ, James CB (2002) Meat refrigeration. CRC Press, Boca Raton, pp 273–275
- Karakolev R (2009) Incidence of *Listeria monocytogenes* in beef, pork, raw-dried and raw-smoked sausages in Bulgaria. *Food Control* 20:953–955. doi:10.1016/j.foodcont.2009.02.013
- Kondjoyan A (2006) A review on surface heat and mass transfer coefficients during air chilling and storage of food products. *Int J Refrig* 29:863–875. doi:10.1016/j.ijrefrig.2006.02.005
- Kondjoyan A, Daudin JD (1997) Heat and mass transfer coefficients at the surface of a pork hindquarter. *J Food Eng* 32:225–240. doi:10.1016/S0260-8774(97)00005-8
- Kuffi KD, Defraeye T, Nicolai BM, De Smet S, Geeraerd A, Verboven P (2016) CFD modelling of industrial cooling of large beef carcasses. *Int J Refrig* 69:324–339. doi:10.1016/j.ijrefrig.2016.06.013
- Kuitche A, Letang G, Daudin JD (1996) Modelling of temperature and weight loss kinetics during meat chilling for time-variable conditions using an analytical-based method—II. Calculations versus measurements on wet plaster cylinders and cast. *J Food Eng* 28:85–107. doi:10.1016/0260-8774(95)00029-1
- Ministerial Decree No. 253 of 15/02/1993 published on “Gazzetta Ufficiale della Repubblica Italiana” No. 173 of 26/07/1993
- Ministerial Provision of 03/03/2014 published on “Gazzetta Ufficiale della Repubblica Italiana” No. 64 of 18/03/2014
- Pham QT, Trujillo FJ, McPhail N (2009) Finite element model for beef chilling using CFD-generated heat transfer coefficients. *Int J Refrig* 32:102–113. doi:10.1016/j.ijrefrig.2008.04.007
- Ramírez CA, Patel M, Blok K (2006) How much energy to process one pound of meat? A comparison of energy use and specific energy consumption in the meat industry of four European countries. *Energy* 31:2047–2063. doi:10.1016/j.energy.2005.08.007
- Rinaldi M, Chiavaro M, Massini R (2014) Mathematical modelling of heat transfer in Mortadella Bologna PGI during evaporative pre-cooling. *Int J Food Eng* 10:233–241. doi:10.1515/ijfe-2014-0023
- Trujillo FJ, Pham QT (2003) Modelling the chilling of the leg, loin and shoulder of beef carcasses using an evolutionary method. *Int J Refrig* 26:224–231. doi:10.1016/S0140-7007(02)00036-1
- World Health Organization (1988) Foodborne listeriosis. World Health Organization, Geneva